

## STRUCTURAL ASPECTS

---

Subjecting the anisotropic network model to a critical examination of its structural features, we identify prevalent patterns of connectivity and relate theoretical and computational results to findings from experiments in the rat's cortex.

### 1.1 INTRODUCTION

Investigation of the brain's connectivity is an ongoing endeavour. Concurrent collaborative efforts like the Human Connectome Project, the Open Connectome Project and the Allen Brain Atlas, intent on mapping the 'wiring' of the brain, as well as the continued development of experimental techniques and computational resources, demonstrate the great interest in advancing this field.

Research in brain connectivity spreads over the whole scale of the brain; from the mapping of fiber pathways between brain regions at the macroscopic level, to the synaptic connections of individual neurons on the microscale, researchers are trying to identify the links that enable the brain its characteristic cognitive abilities. connections, these links are of anatomical nature. However, statistical dependencies and causal relationships between the distinct computational units in the brain are being researched with equal emphasis (Sporns 2007). Connectivity in the context of the anisotropic network model introduced in Section ??, refers in this chapter to structural links. So far, we have only briefly mentioned that the network's nodes should be interpreted as individual neurons; to allow for a discussion of functional relationships between nodes, we have yet to provided a physical description of a neuron's function. Here we explore the network's structural connectivity, modeling synaptic contacts between axon and dendrites of individual neurons.

In the local cortical circuits the anisotropic geometric model was derived from, synaptic connectivity is a major mode of configuration. In those networks, connectivity has been determined to be neither completely random nor exclusively specific; recurring patterns of connectivity have been identified by several reports (Sporns and Kötter 2004; Song et al. 2005; Perin et al. 2011).

HUMAN  
**Connectome**  
PROJECT  
*humanconnectome.org*

*Open Connectome  
Project*  
*openconnectome-  
project.org*

**ALLEN BRAIN ATLAS**  
*brain-map.org*

*synaptic  
connectivity*

The impact of this structural specificity discovered in local networks is shown to be significant; while linking network structure to network dynamics remains an active field of research, several studies were able to employ computational and theoretical models to establish such a connection. A study by Zhao et al. (2011), for example, demonstrates how second order connectivity statistics affect a network's propensity to synchronize. In the same year, Alex Roxin reported on the influence of in- and out-degree distributions on dynamics of neural network (Roxin 2011). Later, Pernice et al. were able to link structural connectivity to spike train correlations in neural networks (Pernice et al. 2011).

Experimentally, paired intracellular recordings are used to determine synaptic connectivity in cortical slices. Using two electrodes, one inserted in the cell and one outside the cell, a single intracellular recording allows for measurement of a cell's membrane potential (Brette and Destexhe 2012, Chapter 3; Weckstrom 2010). Simultaneous recordings from multiple neurons are then able to infer synaptic connectivity by evoking an action potential through current injection in one neuron and observing the change of membrane potential in the other cells (Song et al. 2005).

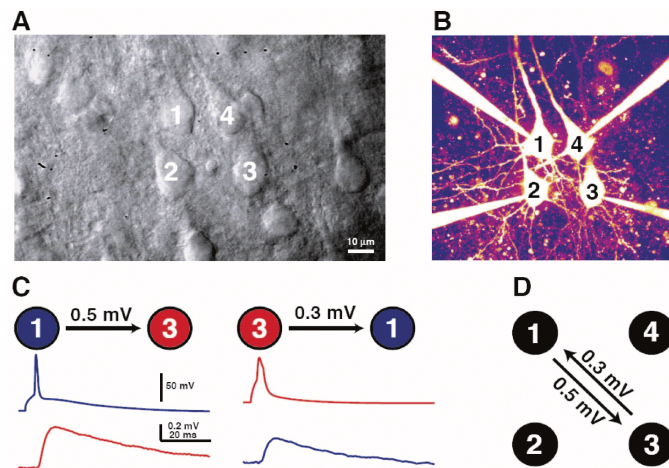


**Figure 1.1:** Song et al. use quadruple whole-cell recordings, observing simultaneously the membrane potential of four neurons. **A)** Contrast image showing four thick-tufted L5 neurons **B)** Fluorescent image of the same cells after patching on **C)** Evoking an action potential in the presynaptic neuron causes characteristic membrane potential change in the postsynaptic neuron **D)** Inferring synaptic connectivity from the EPSP waveform observed in C). Image from Song et al. (2005).

While techniques for paired intracellular recordings are rapidly developing, their ability to capture connectivity patterns of large networks is yet very limited. To this date, the connectome of *C. Elegans* remains

the outstanding exception of a connectivity configuration that has been fully mapped (White et al. 1986). Even in the state-of-the-art experiment conducted by Perin et al., using a setup capable of recording up to twelve neurons simultaneously, the authors note that an investigation of degree distribution was not carried out, due to lack of sufficient data (Perin et al. 2011).

Working with a geometrical network model and its computational implementation, such restrictions disappear; the full information about the network, in form of its connectivity matrix, is given at point in time and can be easily queried for. Experiments that may take days to perform *in vivo*, can be completed in a matter of seconds *in silico*. As such, geometrical models lend themselves to extensive examination of their structural aspects. In trying to exploit these advantages, two approaches present themselves. One may construct a network model that extrapolates the known biological configuration; a full structural examination of these networks could possibly expose relevant patterns not yet observed. For this approach a sophisticated understanding of the biological configuration is critical. Neuron morphology, however, is difficult to describe and extract. For this analysis we suggest a reductionist approach. Having motivated an abstract model reflecting a cortical network’s anisotropy in connectivity, we distinguish emerging structural patterns, specific to anisotropic networks, from results, that only indirectly stem from the network’s anisotropy, in the hopes to be able to characterize the significance of directional heterogeneity in structural connectivity of cortical circuits.

*exploiting the  
benefits of a  
geometrical model*

In this chapter we subject the anisotropic network model introduced in Section ?? to a critical analysis of its structural aspects. General network topology, as well as specific modes and patterns of connectivity, are to be identified and laid out for comparison with findings in biological neural networks. In an effort to identify structural features that can be directly associated with the network’s anisotropy in connectivity, it is crucial to differentiate such findings from results that are only indirectly caused by the network’s anisotropy. To this end we are recruiting the different network types introduced in the previous chapter throughout this analysis. Having shown a decreasing degree of anisotropy in rewired and distance-dependent networks, both models will serve as reference to compare against for structural features found in anisotropic networks. Analyzing standard graph measures in the first two sections, we quickly move on to towards neuronal network specific connectivity and anisotropy’s role in being able to model such highly non-random patterns in the later sections.

*rewired and  
distance-depen-  
dent networks as  
reference*

## 1.2 DEGREE DISTRIBUTION

*cf. Definition ??*

The in- and out-degree of a vertex in a directed graph describes the number of incoming and outgoing connection from and to other vertices. As a fundamental concept in graph and network theory, the degree distribution is integral in the categorization of networks and allows for the estimation of graph properties.

Node degree distribution was shown to have strong impact on the dynamics of neuronal networks models commonly used in computational neuroscience research (Roxin 2011). Increasing in-degree variance for example could be connected to the appearance of oscillations in the network. Extracting degree distributions from biological networks however, remains a challenge as many neurons need to be tracked simultaneously to obtain enough data to confidently estimate degree distributions.

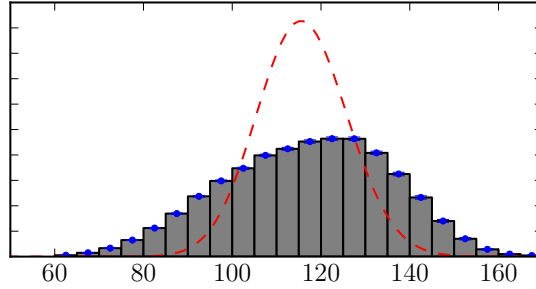


**Figure 1.2: In-degree distribution in anisotropic networks shows comparably high variance and is skewed to the left** From 250 anisotropic networks in-degree distributions were extracted and are shown in a normed histogram plot, errorbars SEM. Comparison with the binomial degree distribution (red) of a Gilbert random graph model with matching parameter set ( $N = 1000$ ,  $p = 0.116$ ) shows higher variance of in-degrees in anisotropic networks (sample variance = 344.54, variance of binomial distribution  $Np(1-p) = 102.44$ .) Skewness to the left of the sample is  $-0.1763$ . (9326138e)

Here we analyze in- and out-degrees in the anisotropic network model. First we find that compared to the binomial in-degree distribution of a Gilbert random graph model, in-degrees of vertices in anisotropic networks display higher variance and their distribution is skewed to the left (Figure 1.2). However, this specific in-degree profile is not an intrinsic property of anisotropy, as the distribution remains stable under manipulation of the anisotropy degree and closely matches the profile of a purely distance-dependent network (Figure 1.3). This result agrees with findings of Perin et al. (2011, Fig. S3), who were able to recreate

degree distributions from their experiment with layer 5 thick-tufted pyramidal cells in neonatal rats from the extracted distance-dependent connection profiles alone.

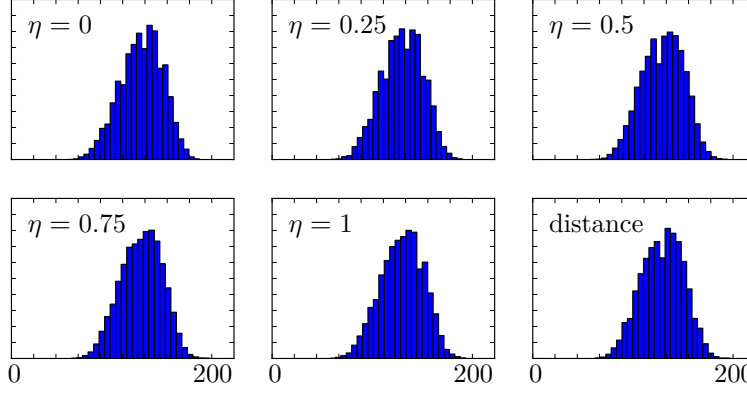


**Figure 1.3: In-degree distribution not affected by varying degrees of anisotropy** In-degree distributions from the 25 sample graphs and their rewiring stages are plotted in normed histograms and listed from rewiring factor  $\eta = 0$  (original anisotropic) to  $\eta = 1$  (completely rewired, maximal isotropy). Comparison shows that varying degrees of anisotropy do not influence the degree distribution, in fact in-degree distributions match with the degree distribution of an equivalent distance-dependent network shown bottom-right (77995b6b).

While the out-degree distribution of vertices in the anisotropic network also shows itself stable under rewiring, its distribution is drastically different from the out-degree distribution in a comparable distance-dependent network (Figure 1.4). The asymmetric, long-tailed distribution is identified as an artifact of the anisotropic network’s spatial confinement; a neuron, closely located near a surface edge, might have an axon projection out of the square causing minimal out-degree or, projecting through the entire length of the surface, may have maximal out-degree. Approximating the expected number of outgoing connections for a vertex in an anisotropic network of size  $N$ , side-length  $s$  and axon width  $w$  as

$$N \frac{wl}{s^2},$$

with parameters  $N = 1000$  and  $\frac{w}{s} = 0.252$ , we obtain an upper bound for the expected out-degree,

$$N \frac{wl}{s^2} \leq N \frac{w}{s} \sqrt{2} \approx 350.$$

If  $f(l)$  is the probability density function to find axon length  $l$  for a random node  $v$  in the anisotropic network model, the out-degree distribution is then approximated by

$$\mathbf{P}(d_{\text{out}}(v) = N \frac{wl}{s^2}) = f(l), \quad (1.1)$$

see also [Figure 1.5](#).

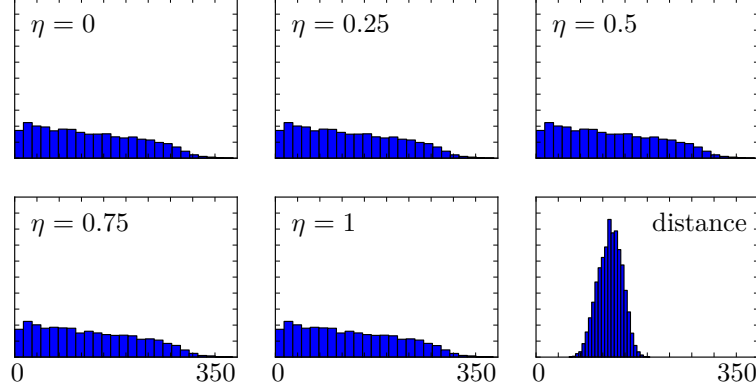


**Figure 1.4: Out-degree distribution not affected by varying anisotropy but highly different from distance-dependent networks** Out-degree distributions from the 25 sample graphs and their rewiring stages are plotted in normed histograms and listed from rewiring factor  $\eta = 0$  (original anisotropic) to  $\eta = 1$  (completely rewired, maximal isotropy). While varying degrees of anisotropy do not influence the degree distribution, the characteristic out-degree profile is drastically different from the distribution found in equivalent distance-dependent networks (77995b6b).

*Steep incline for  
small out-degree  
cut off due to  
binning (cf. ??)*

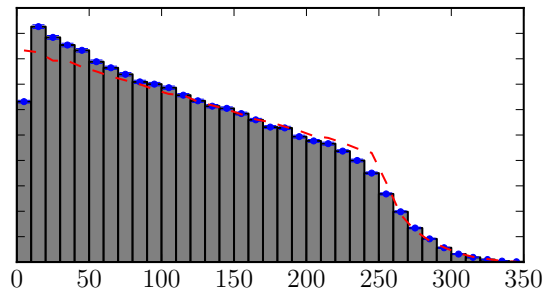


**Figure 1.5: Characteristic out-degree distribution as an artifact of network's boundaries** From 250 anisotropic networks out-degree distributions were extracted and are shown in a normed histogram plot, errorbars SEM. The characteristic distribution is identified as an artifact of the network's spatial confinement; using equation 1.1 the out-degree profile is approximated (red) by the distribution of axon lengths in the anisotropic network (019555b0).

### 1.3 SMALL WORLD PROPERTIES

Small-world networks, as described in Section ??, are characterized by a small average path length and comparably high clustering coefficient. In brain networks, combining advantages of sparse connectivity with mostly local and only few long-range projections, small-world properties are frequently discussed as a way of achieving high efficiency in the parallel processing of information (cf. Achard and Bullmore 2007). While most often reported on the macroscale (Sporns and Zwi 2004; Bassett and Bullmore 2006), small-worldness is also found in local cortical networks (Perin et al. 2011, SI).

Here we are interested in exploring the question whether anisotropy in connectivity influences the small-worldness of geometric networks. First we find that at a network size  $N = 1000$ , anisotropic networks display a relatively high clustering coefficient,  $c = 0.1581 \pm 0.0008$  compared with  $p = 0.116$  in random networks, and a comparable path length,  $l_{\text{aniso}} = 1.937 \pm 0.002$  and  $l_{\text{random}} = 1.8820 \pm 0.0001$ , ascertaining a small-world property in the anisotropic network model.

*in random  
networks from  
independence  
clustering =  $p$*

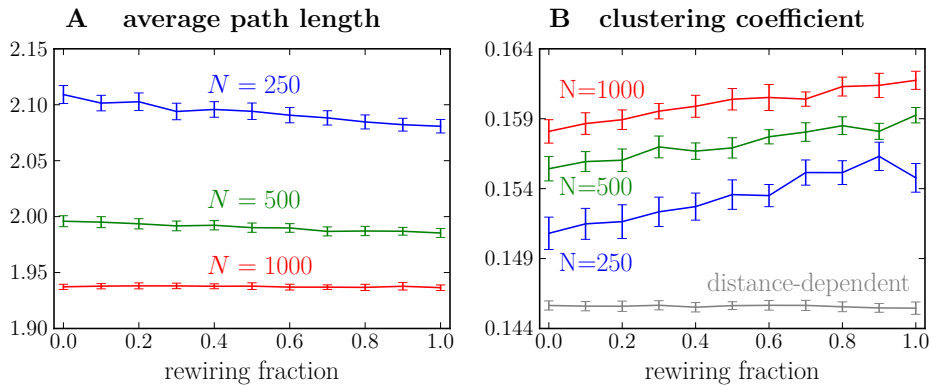


**Figure 1.6: Anisotropy does not contribute to small-worldness** In increasingly rewired networks, trends show a decreasing average path length and rising clustering coefficient and thus possibly a higher degree of small-worldness in the rewired, isotropically connected networks. **A)** Average path lengths for network sizes  $N = 250, 500$  and  $1000$ , where vertex pairs with no existing are discarded. Individual value pairs are obtained by averaging over a trial size of 20, 15 and 5 respectively; errorbars are SEM. **B)** Network configuration as in A), additionally showing clustering coefficients for distance-dependent networks. (064f9b10)

However, is this degree of small-worldness inferred by anisotropy in connectivity? Using distance-dependent networks as a reference, we find that successively eliminating anisotropy through rewiring contributes

positively to the small-world property; with rising isotropy in the network, the characteristic path length declines in small networks and remains unchanged in larger networks, while the clustering coefficient increases regardless of network size, resulting together in rewired networks to display a higher degree of small-worldness (Figure 1.6).

In distance-dependent networks the average path length is generally smaller than in (rewired) anisotropic networks (??), matching those of a random network as reported above. At the same time also the clustering coefficient is smaller than in anisotropic networks (Figure 1.6), resulting overall in a comparable degree of small-worldness in distance-dependent networks <sup>1</sup> and leading to the conclusion that the observed small-worldness in the anisotropic networks is due to the imposed distant-dependent connectivity rather than the anisotropy in connectivity.

#### 1.4 TWO NEURON CONNECTIONS

Connectivity in local cortical circuits exhibits a salient feature: Examining the occurrence of connections in neuron pairs, studies have repeatedly found that bidirectionally connected neuron pairs appear much more frequently than expected from the network’s overall connection probability. In layer 5 of the somatosensory cortex studies from Markram (1997) and Perin et al. (2011) have found an overrepresentation of reciprocally connected pairs of thick tufted pyramidal cells, an observation that has also been reported in layer 2/3 (Holmgren et al. 2003) and layer 5 (Song et al. 2005) of the visual cortex. The overrepresentation of bidirectionally connected pairs is significant, Song et al. for example found such pairs represented four times the expected amount.

The underlying connection principle imposing this overrepresentation on the network however remains unclear. Song et al. discuss the possibility of known learning rules to explain their findings, leaving a definitive answer open to further investigation. More recent studies find overrepresentation of reciprocally connected pairs *in vitro* resulting from functional specificity (Ko et al. 2011) and *in silico* from dense neuron clustering rules (Klinshov et al. 2014), identifying specific network characteristics that may contribute to the reported overrepresentation *in vivo*.

---

<sup>1</sup> Differences in the absolute values of both path length and clustering coefficient presumably relates to difference in the out-degree distribution (Figure 1.4)



Here we examine anisotropy in connectivity as a possible candidate for an underlying principle explaining the characteristic two neuron connection distribution. In random networks, the chance to encounter a specific mode of connection in a random pair of neurons can easily be computed from the overall connection probability  $p$ . For this let  $X$  be the random variable of the number of edges between two different vertices in a Gilbert graph  $G(n, p)$  with  $n \geq 2$ . As the edges are independently realized, resulting in a simple directed graph, we have

$$\begin{aligned}\mathbf{P}(X = 0) &= (1 - p)^2 && \text{unconnected pair,} \\ \mathbf{P}(X = 1) &= 2p(1 - p) && \text{single connection,} \\ \mathbf{P}(X = 2) &= p^2 && \text{reciprocal connection;}\end{aligned}\tag{1.2}$$

in short  $\mathbf{P}(X = k) = \mathcal{B}_{2,p}(k)$  for  $k \in \{0, 1, 2\}$  and  $\mathbf{P}(X = k) = 0$  otherwise. Using this probability distribution as the expectation for connectivity of neuron pairs in the various network types, a numeric analysis of the anisotropic sample graphs reveals that bidirectionally connected pairs appear almost twice as often as expected from the overall connection probability ( $p = 0.116$ ) and equations 1.5, similarly as reported by Song et al. (Figure 1.7 A). However, comparing the pair probabilities in anisotropic networks with the probabilities in their rewired counterparts, we find that anisotropy does not influence the occurrence of two-neuron motifs (Figure 1.7 B) In fact, expected connections in neuron pairs are identical in distance-dependent and rewired anisotropic networks (??).

We further support this observation by computing the probability distribution for the expected number of edges between two random vertices in the anisotropic graph model. For this we assume that only the distance-dependent connection probability  $C(x)$  determines the occurrence of edges in vertex pairs in the anisotropic graph model. Then, using the probability distribution  $f(x)$  for the a random neuron pair to be at distance  $x$ , we calculate

$$\begin{aligned}\mathbf{P}(X = 0) &= \int_0^{\sqrt{2}} (1 - C(x))^2 f(x) dx, \\ \mathbf{P}(X = 1) &= \int_0^{\sqrt{2}} 2C(x)(1 - C(x)) f(x) dx \quad \text{and} \\ \mathbf{P}(X = 2) &= \int_0^{\sqrt{2}} C(x)^2 f(x) dx.\end{aligned}$$

Inserting the distance-dependent connection probabilities  $C(x)$  in the anisotropic graph model as computed in Theorem ?? and the probability distribution  $f(x)$  from Theorem ?? we obtain

$$\begin{aligned} \mathbf{P}(X = 0) &= 0.791336 & 0.7907 \pm 0.0008 \\ \mathbf{P}(X = 1) &= 0.184151 & 0.1846 \pm 0.0007 \\ \mathbf{P}(X = 2) &= 0.024513 & 0.02462 \pm 0.00009, \end{aligned}$$

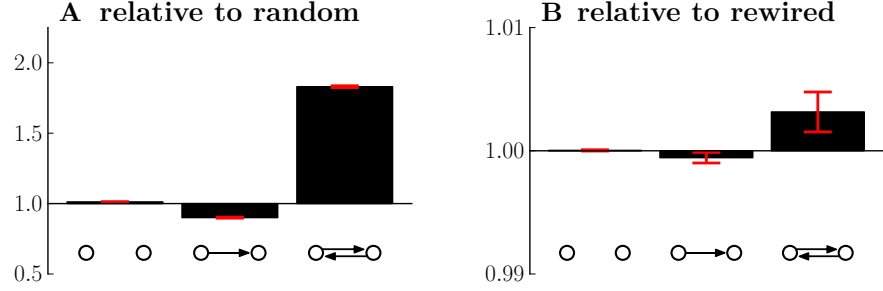


**Figure 1.7: Overrepresentation of reciprocal connections in anisotropic networks due to distance-dependent connectivity** Extracting the counts of unconnected, one-directionally and bidirectionally connected neuron pairs in the anisotropic sample graphs, overrepresentation of reciprocally connected pairs is identified as a feature of the network’s distance dependency as opposed to anisotropy in connectivity. **A)** Showing the quotient of the counts for the three pair types, extracted from the set of sample graphs, with the number of expected pairs in Gilbert random graphs  $G(n, p)$ , where  $n = 1000$  and  $p = 0.116$  were matched to the sample graph parameters. While single connections appear less often than in Gilbert random graphs, reciprocal connections are significantly overrepresented. Errorbars SEM. **B)** Comparing appearance of connection pairs in the anisotropic sample graphs with their respective appearance in the rewired sample graphs, we find that eliminating anisotropy does not significantly change the counts for the connection types, indicating that anisotropy does not influence two neuron connection probabilities. Errorbars SEM. (c5f1462b)

perfectly matching the probabilities extracted from anisotropic sample graphs in the right column (error SEM, c5f1462b). Noting that distance-dependency alone is sufficient to accurately predict edge probabilities in neuron pairs in the anisotropic network model and combined with the observations in Figure 1.7, we conclude that varying degrees of anisotropy do not affect the occurrence of neuron pair motifs.

The discussion in the last section focused on the effect of anisotropy in connectivity on the occurrence of neuron pair motifs. Could distance-dependency itself, as imposed by the specific geometry, be a decisive factor in the distribution of edge counts in neuron pairs? [Song et al. \(2005\)](#), as well as [Perin et al. \(2011\)](#), report an overrepresentation of reciprocal connections independent from distance-dependent connectivity, opposing the observations made in the last section ([Figure 1.7 A](#)). Furthermore, the connectivity profile in the anisotropic graph model, as identified in Section ??, follows purely from abstract geometry rather than being motivated by connectivity found in cortical circuits. In an attempt to rectify this and to allow for a more differentiated examination of two neuron connections, in this section we step away from simplistic geometry and “tune” the anisotropic networks to display a distance-dependent connectivity as reported by Perin et al. by adjusting the width  $w(x)$  at any point  $x$  along the axon’s projection.

For this we introduce anisotropic networks tuned to reflect a given distance-dependent connection profile  $C(x)$ . We are facing the following problem: Given  $C(x) : [0, \sqrt{2}) \rightarrow [0, 1]$ , find  $w : [0, \sqrt{2}) \rightarrow [0, \infty)$  such that the probability to have a connection from  $v_1$  to  $v_2$  for arbitrary vertices  $v_1 \neq v_2$  in an anisotropic graph  $G(n, w)$  with distance  $d(v_1, v_2) = x$  is  $C(x)$ . The problem is in general highly complex when nothing can be assumed about  $C(x)$ . We find an approximate solution to the problem considering the following geometric relation:

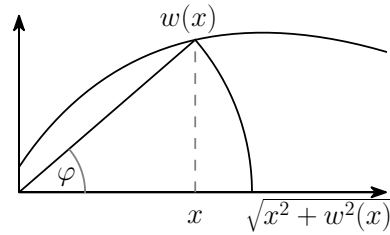


**Figure 1.8:** Computing connection probability  $C(x)$  from non-constant  $w(x)$

From [Figure 1.8](#) we have the relation

$$C\left(\sqrt{x^2 + w^2(x)}\right) = \frac{1}{\pi} \arctan \frac{w(x)}{x}. \quad (1.3)$$

In order to solve for  $w(x)$  we first consider a linear approximation, expanding

$$C\left(\sqrt{x^2 + w^2(x)}\right) \approx C(x) + \left(\sqrt{x^2 + w^2(x)} - x\right) C'(x).$$

The resulting transcendental equation

$$C(x) + \left( \sqrt{x^2 + w^2(x)} - x \right) C'(x) = \frac{1}{\pi} \arctan \frac{w(x)}{x}$$

is however still too complex in the context of this work. Instead we propose the approximation  $\sqrt{x^2 + w^2(x)} \approx x$ , which inserting into 1.3 yields

$$C(x) \approx \frac{1}{\pi} \arctan \frac{w(x)}{x}. \quad (1.4)$$

Under the assumption that  $C(x) < \frac{1}{2}$  for all  $x$  we obtain the identity

$$w(x) = x \tan(\pi C(x)), \quad (1.5)$$

being aware that it only holds as well as approximation 1.4 does.

Here we use relation 1.5 to generate anisotropic networks reflecting the distance-dependent connectivity profile as found by Perin et al. (2011). For this we finally need to adjust the before arbitrarily determined side length of the network's surface. Perin et al. mapped connectivity in layer 5 of the rat's somatosensory cortex up to a distance of 300  $\mu\text{m}$ . Using this reported distance connectivity to generate anisotropic networks via 1.5, the chosen side length  $s$  determines the networks overall connectivity (Figure 1.9 A). We determine  $s = 296 \mu\text{m}$  to match the overall connection probability of  $p = 0.116$  as used before and reported by Song et al. (Figure 1.9 B). The obtained value for  $s$  is consistent with the slice thickness of 300  $\mu\text{m}$  used in Perin et al.'s experiment.

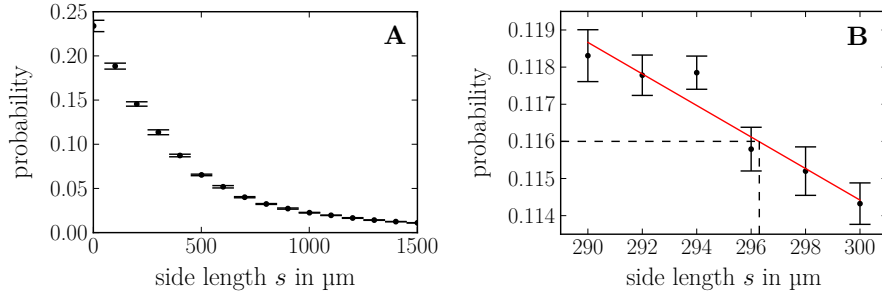


**Figure 1.9: Network side length adjusted to match overall connection probability** Side length of the network's surface determines the overall connection probability in the network when axon width function  $w(x)$  is fixed. **A)** Connection probability declines with rising side length **B)** Determining side length as  $s = 296 \mu\text{m}$  to match  $p = 0.116$  as reported by Song et al. (2005). (6154302f, ef0e785d)

Having determined the network's side length  $s$ , we're extending the quiver of generated sample networks for the numerical analysis once more by the "tuned anisotropic graphs", in which the axon width

$w(x)$  was determined such that the networks reflect Perin’s connectivity profile. Analyzing the obtained axon width function we note that  $x \gg w(x)$  holds for most  $x$ , justifying the approximation

$$\sqrt{x^2 + w^2(x)} \approx x$$

*a posteriori* (Figure 1.10). From the 25 generated networks overall connection probability is extracted as  $p = 0.1160 \pm 0.0006$  (SEM), as expected from the choice of  $s$  (f11dca65).

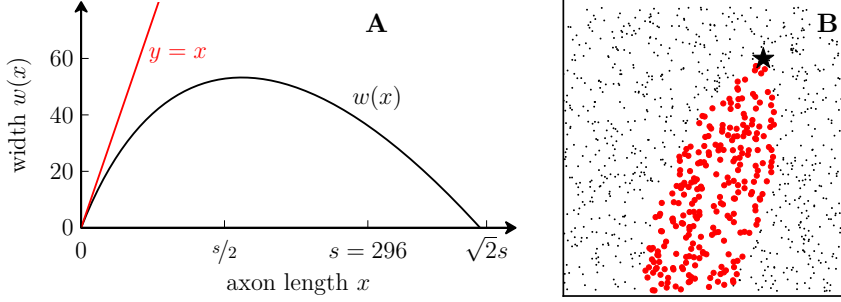


**Figure 1.10: Anisotropic network model with tuned axon width  $w(x)$**  **A)** Resulting axon width function  $w(x)$  from tuning to distance-dependent connection profile as reported by Perin et al. (2011), see also Figure 1.11. Note that  $x \gg w(x)$  for most  $x$ , supporting approximation 1.4. **B)** Showing for a single neuron (star) connected (red) and unconnected (gray) neurons in the tuned anisotropic network, revealing the characteristic axon shape. (d45c02e4, 8f0d65e4)

Overall distance-dependent connection probabilities in the tuned anisotropic graphs clearly match the profile of Perin et al. (Figure 1.11 A), presenting strongest the argument in support of the chosen approximation. Analyzing two neuron connections in the tuned networks, we affirm the findings of the last section. In their experiment, Perin et al. were able to show an overrepresentation of reciprocal connections at any inter-neuron distance (Figure 1.11 B-C). Rather than matching these profiles, we find that occurrences of one- and bidirectionally connected pairs in the anisotropic graphs align with probabilities obtained from the distance-dependent overall connection probability  $p(x)$  under the assumption of independence (cf. Equation 1.5),

$$\begin{aligned} \mathbf{P}_{X=1}(x) &= 2p(x)(1 - p(x)) && \text{single connection,} \\ \mathbf{P}_{X=2}(x) &= p(x)^2 && \text{reciprocal connection.} \end{aligned}$$

Thus, in comparison with Perin et al.’s findings, we find that anisotropy in connectivity cannot account for the overrepresentation in reciprocal connections. While results in Section 1.4 still indicated such an overrepresentation due to distance-dependency, examining the occurrence of two neuron connections at any inter-neuron distance in anisotropic

revisiting two  
neuron  
connections

networks, tuned to a distance-dependent connection profile matching experimental findings from cortical circuits, imply complete unrelatedness of anisotropy and two-neuron connection distributions.

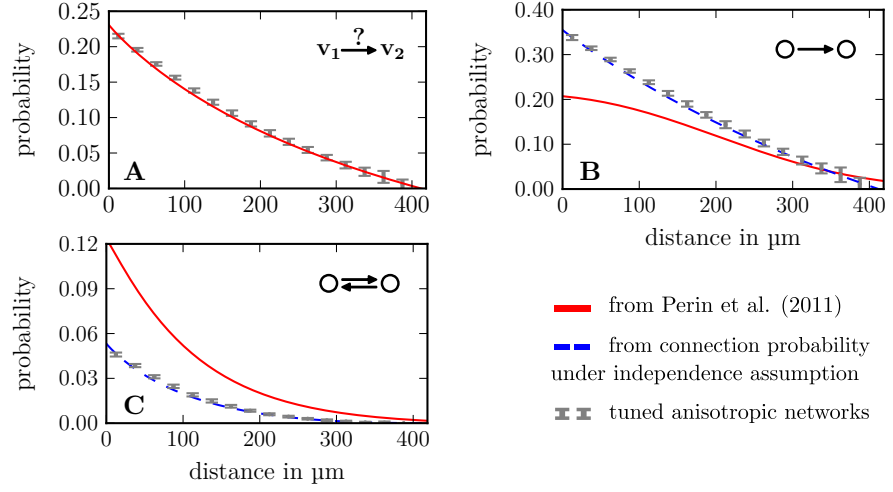


**Figure 1.11: Distance-independent overrepresentation of reciprocal connections** Comparison of occurrences of one- and bidirectionally connected neuron pairs in the tuned anisotropic networks (gray) with profiles found by Perin et al. (red), shows that overrepresentation of bidirectional pairs is distance-independent and not connected to anisotropy. **A)** Overall connection probability in the tuned anisotropic networks was successfully adjusted to reflect connection probability found by Perin et al. **B)-C)** Showing in blue the probabilities to obtain a neuron pair motif (single edge in B, two edges in C) calculated under independence assumption from the overall probability from A), we find that counts in the tuned anisotropic networks (gray) match the independence assumption and do *not* show the overrepresentation present in Perin et al.'s experiment. (875505b0)

## 1.6 MOTIFS

Non-random connectivity in local cortical circuits extends well beyond specific connection probability in neuron pairs: As one of their main results, Song et al. (2005) report a characteristic occurrence of motifs of three neurons, while Perin et al. (2011) find patterns in the number of connections appearing in clusters of up to 8 neurons. Motifs have been shown to have a significant influence on network dynamics, with patterns affecting dynamical correlations (Pernice et al. 2011) and network synchrony (Zhao et al. 2011).

Finding no correlation between two-neuron connection probabilities and anisotropy in connectivity prior, does anisotropy influence the occurrence of neuron motifs? In this section we analyze higher order connectivity in the different network types and observe a surprisingly strong impact of anisotropy on patterns of connected neurons, promoting the concept as an underlying principle for non-random network connectivity.

### *Three-neuron patterns*

We first investigate the occurrence of three-neuron patterns in anisotropic networks. Song et al. (2005) reported a characteristic, highly non-random motif distribution of pyramidal cells in the rat's visual cortex layer 5, a result later confirmed by Perin et al. (2011) in their experiment in the rat's somatosensory cortex layer 5. Repeating the experiment *in silico* for the different networks subject to this study, we find similar, characteristic motif distributions strongly influenced by anisotropy in connectivity.

There are  $13^2$  non-isomorphic 3-motifs in simple directed graphs. In reference to Song et al.'s result, the patterns are labeled 4 to 16,



Let  $X$  be a random variable that maps three random vertices  $v_1 \neq v_2 \neq v_3$  in a graph  $G$  to the  $n \in \{4, 5, \dots, 16\}$  labeling the isomorphism class of the full subgraph with vertex set  $\{v_1, v_2, v_3\}$  in  $G$  as above if the subgraph is connected, and let  $X$  map to  $n = 0$  otherwise. A first idea of how to compute the distribution of  $X$  is by inferring the probabilities of motif occurrence from the two-neuron connection probabilities from Section 1.4. In anisotropic networks we found that the probabilities of occurrence are

$$\begin{aligned} p_u &= 0.791336 && \text{for unconnected pairs,} \\ p_s &= 0.184151 && \text{for single connections and} \\ p_r &= 0.024513 && \text{for reciprocal connections.} \end{aligned}$$

From these we may, for example, calculate the probability of occurrence for motif 8,

$$\mathbf{P}(X = 8) = 6 p_u p_s p_r,$$

<sup>2</sup> There are 16 non-isomorphic simple directed graphs with 3 nodes. Three of those graphs are unconnected (cf. Davis 1953, N. J. A. Sloane. The On-Line Encyclopedia of Integer Sequences, <http://oeis.org>. Sequence A000273).

where the factor 6 is determined by the number of different *labeled* graphs belonging to the isomorphism class. The distribution of  $X$  for the remaining motifs is given by

$$\begin{aligned} \mathbf{P}(X = 4) &= 3p_s^2p_u & \mathbf{P}(X = 9) &= 3p_r^2p_u & \mathbf{P}(X = 13) &= 6p_s^2p_r \\ \mathbf{P}(X = 5) &= 3p_s^2p_u & \mathbf{P}(X = 10) &= 6p_s^3 & \mathbf{P}(X = 14) &= 3p_s^2p_r \\ \mathbf{P}(X = 6) &= 6p_s^2p_u & \mathbf{P}(X = 11) &= 2p_s^3 & \mathbf{P}(X = 15) &= 6p_s p_r^2 \\ \mathbf{P}(X = 7) &= 6p_s p_u p_r & \mathbf{P}(X = 12) &= 3p_s^2p_r & \mathbf{P}(X = 16) &= p_r^3. \end{aligned}$$

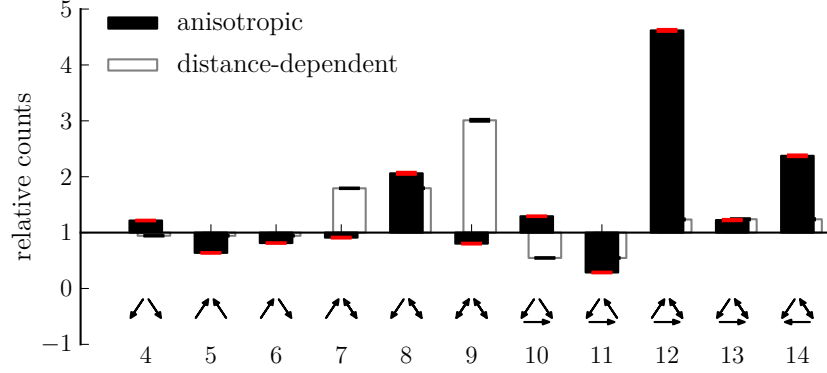


**Figure 1.12: Relative occurrence of three-neuron patterns** Extracting the counts of three-node motifs in anisotropic (filled bars) and distance-dependent networks (unfilled bars), the quotient of the obtained count with the number of occurrences expected from the two-neuron connection probabilities in the networks (cf. Section 1.4) shows the over- and underrepresentation of specific motifs in the network (red and black errorbars are SEM). In anisotropic networks pattern 12, for example, appears around five times more often than we would expect from the occurrence two-neuron connections. The relative counts for anisotropic networks resemble the findings of [Song et al. \(2005\)](#) and differ significantly from the counts in distance-dependent networks, implying that anisotropy has a strong influence on the relative occurrence of three-neuron patterns. (4839ce41)

distribution from  
neuron-pairs as  
reference

Does this distribution accurately reflect the occurrences of three-neuron motifs in anisotropic or even distance-dependent networks? Here we take the distribution determined from the two-neuron probabilities as a reference to analyze occurrences of three-neuron motifs in our sets of sample graphs. Counting the occurrences of patterns in we find that there are significant over- and underrepresentations in anisotropic as well as distance-dependent networks, relative to our expectation ([Figure 1.12](#)). We find, for example, that in anisotropic graphs pattern 12 occurs almost 5 times as often as we would have expected from the two-neuron probabilities, whereas the counts for pattern 11 only make up less than 30% of the occurrences expected.



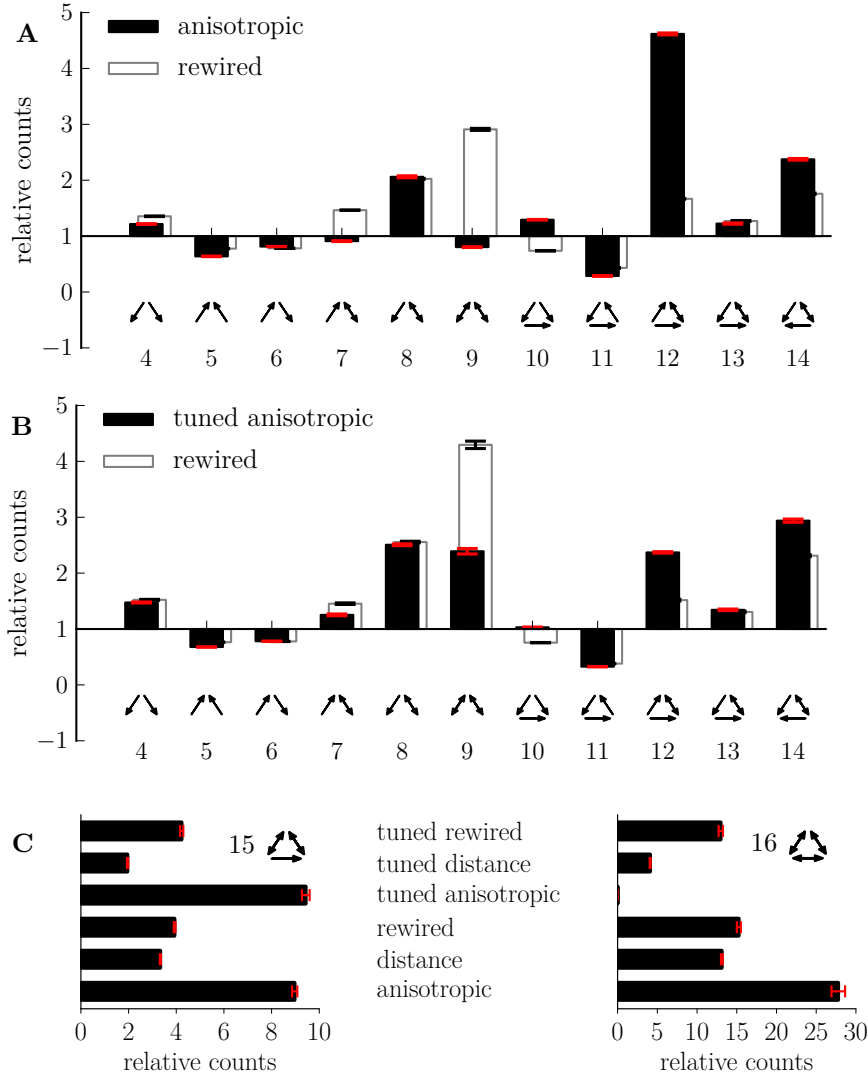


**Figure 1.13: Three-neuron motif occurrence in different network types** **A)** Comparing counts in anisotropic sample graphs with their rewired counterparts. **B)** Three-neuron motifs occurrence in tuned anisotropic networks (cf. Section 1.5) with their rewired counterparts. For this two-neuron connection probabilities were extracted as in Section 1.4 and motif probabilities were calculated analogously to anisotropic networks. **C)** Relative counts for the high edge count motifs 15 and 16 for different network types, errorbars SEM. (4839ce41)

Comparing the relative counts for motifs in anisotropic graphs with those in comparable distance-dependent networks, we identify a strong influence of anisotropy in connectivity on three-neuron motif occurrence (Figure 1.12). In their experiments, Song et al. and Perin et al. find an overrepresentation of motifs 4, 10, 12 and 14. In anisotropic networks increased counts of motifs 4, 8, 10, 12, 13 and 14 were recorded. However, motifs 8 and 13 are overrepresented in distance-dependent

*anisotropy  
strongly affects  
3-motif occurrence*

networks as well, leaving the reported motifs 4, 10, 12 and 14 as motifs that are overrepresented due to anisotropy. To analyze this effect closer, we also compare three-neuron counts before and after rewiring in anisotropic networks (Figure 1.13).

Considering motif occurrences in anisotropic as well as tuned anisotropic networks, we once again confirm the overrepresentation of motifs 4, 10, 12 and 14. However, increased counts of pattern 4 are observed in the rewired networks as well, leading to the conclusion that increased occurrence in this motif is only implicitly affected by anisotropy. Motifs 10, 12 and 14 however show significant overrepresentation even over their rewired counterparts in anisotropic as well as in tuned anisotropic networks.

The overall motif distribution shows itself stable under changes in the distance-dependency with the notable exception of motif 9, that shows underrepresentation only in anisotropic but not in tuned anisotropic or any distance-dependent network type. Analyzing the occurrences of motifs 15 and 16 with a high edge counts (Figure 1.13 C) we find that anisotropy has strong influence on both motifs, with motif 15 being significantly overrepresented in anisotropic networks. Motif 16 shows a highly increased occurrence in anisotropic networks, however tuning causes the loss of this feature in the network connectivity.

#### *results summary*

Summarizing the above observations, we find that anisotropy in connectivity induces increased occurrence of motifs 10, 12, 14 and 15 in the network, reflecting experimental results in the rat's cortex. While over- and underrepresentation observed in local cortical circuits can be indirectly linked to anisotropy for some motifs (4, 9), it does not accurately reflect observed counts for other motifs (8) and shows instability under manipulation of distance-dependency in some patterns (9, 16).

#### *Edge counts in neuron clusters*

In motifs consisting of 3 to 8 neurons, Perin et al. (2011) reported a striking statistic from their experiment with pyramidal cells in the rat's somatosensory cortex, layer 5: Counting the number of edges appearing in a cluster of  $n$  neurons, they find that clusters with relatively high edge counts appear significantly more often than expected from the network's distance-dependent connection probabilities alone. Do anisotropic networks exhibit a similar feature?

Recruiting the collection of sample graphs once again we analyze the occurrence of edge counts in clusters of  $n$  neurons in the different net-

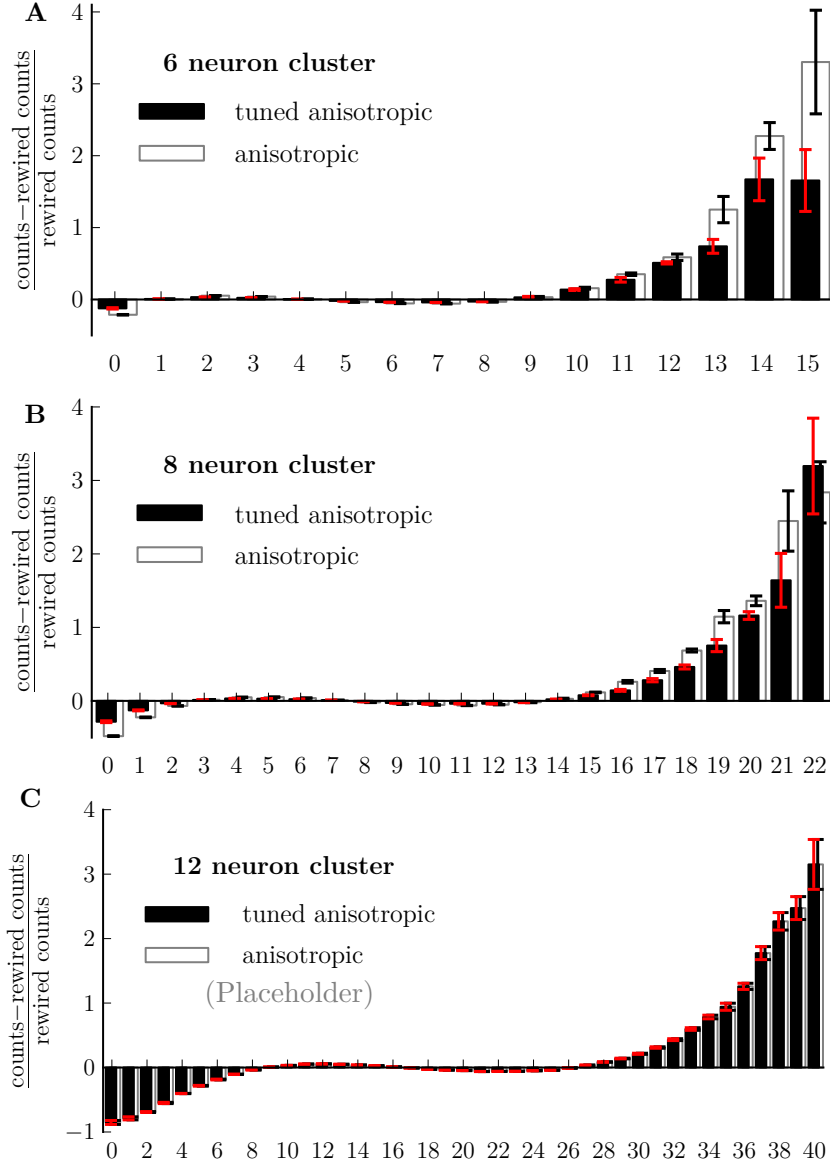


**Figure 1.14: High edge counts are overrepresented in networks with anisotropy** Normalized difference between number of edges in clusters of 6, 8 and 12 randomly selected neurons in anisotropic networks and rewired networks shows an overrepresentation of high edge counts in networks with anisotropy in connectivity. Errorbars SEM. (??)

work types. In the main process, after randomly sampling  $n$  pairwise different vertices  $S_n$ , the motif  $H$  in  $G$  with vertex set  $V(H) = S_n$  is identified and its number of edges  $|E(H)|$  is recorded. Repeating this sufficiently often (order  $10^6$ ) we obtain edge counts for clusters of 6,8 and 12 neurons in the anisotropic- and tuned anisotropic networks as well as in their rewired counterparts. Then, showing the difference between counts in the anisotropic networks and counts in the rewired networks, normalized by the rewired counts, we identify an overrep-

representation of high edge counts in the neuron similar to Perin et al. (Figure 1.14).

In anisotropic networks an overrepresentation of high edge counts is found consistently through clusters of 6, 8 and 12 neurons, with the highest counts appearing up to four times as often as expected. Low edge counts occur less frequently than expected and an increasing number of connections shows an oscillation around the expectation. These findings are consistent with the report of Perin et al, which however indicates a higher maximal overrepresentation in clusters of 8 neurons.

Tuning the network’s distance-dependency appears to not affect the overrepresentation as edge counts in anisotropic and tuned anisotropic essentially match (Figure 1.14). Anisotropy in connectivity therefore presents itself as an important factor in the occurrence of increased high edge counts in cortical networks, possibly fully reflecting the findings of Perin et al., as the overrepresentation effect is found to be even stronger when comparing edge counts to distance-dependent networks as opposed to rewired versions (Figure 1.15).

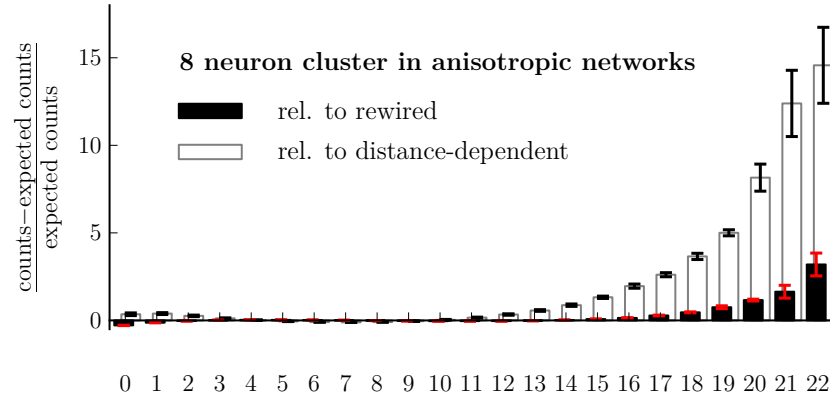


**Figure 1.15: Stronger overrepresentation of clusters with high edge counts with distance-dependent networks as reference**  
 Showing the occurrence of edge counts in clusters of 8 random neurons, we find that the overrepresentation of motifs with high edge counts is stronger when taking distance-dependent networks as a reference as opposed to rewired networks. (7c826e10)

## 1.7 COMMON NEIGHBOR RULE

In their study, Perin et al. follow their report of increased edge counts in neuron clusters with the observation of a “common neighbor rule”: Relying once again on their data in the rat’s somatosensory cortex, Perin

et al. find that not only do neuron pairs with a high number of common neighbor count appear significantly more often than expected, but also that such pairs display a higher probability of being connected. In fact, the relationship between pair connectivity and number of common neighbors appears to be linear. Perin et al. also report that this effect is most pronounced when only considering common in-neighbors, that is other neurons that are projecting to both neurons in the pair.

*common neighbor rule as underlying principle?*

Here we also investigate our networks for the existence of such a common neighbor relationship. Simultaneously recording connection probabilities and the number of common neighbors between pairs of neurons, we find inherent dependencies between the two quantities in all network types (Figure 1.16).

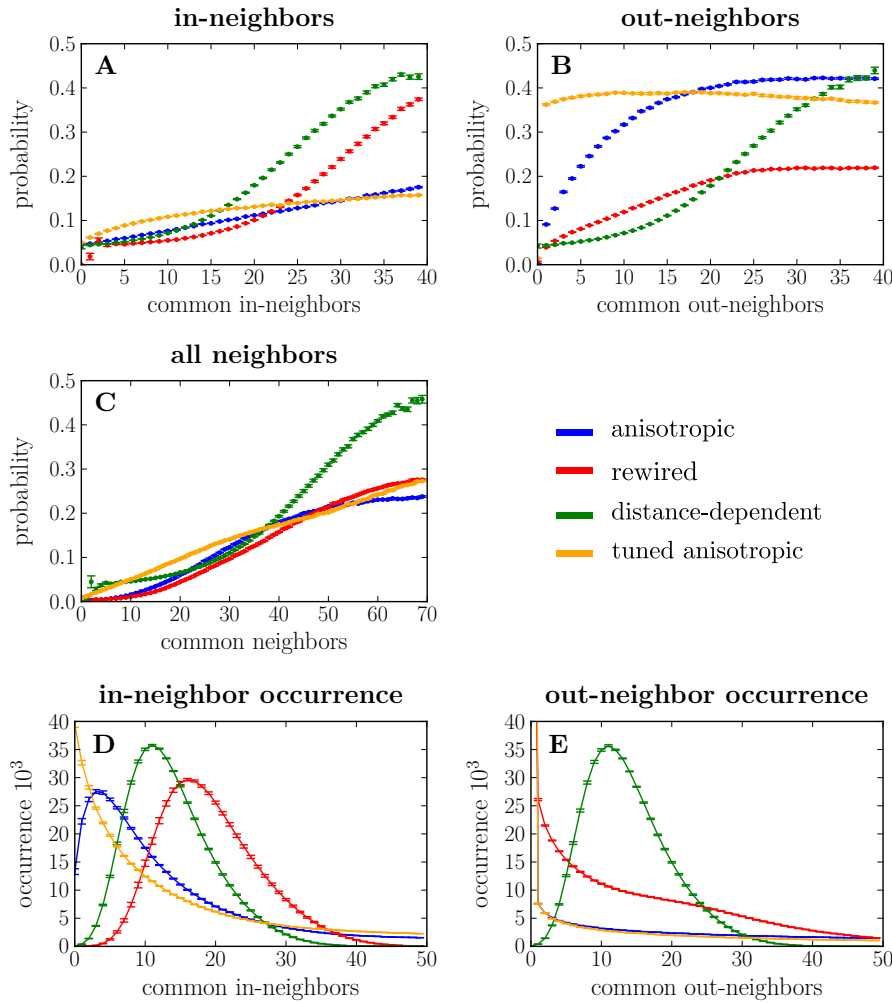


**Figure 1.16: Common neighbor rules in the different network types**  
Showing the dependency of connection probability on the number of shared neighbors for random neuron pairs, characteristic curves for the network types (see legend) arises. High error margins (errorbars SEM) for small number of common neighbors in distance-dependent networks is induced by vanishingly low occurrence of a small common neighbor count. (5841710e)

Analyzing the results, we immediately note the sharp difference between in- and out-neighbors in their effect on connection probabilities in anisotropic networks, as well as in rewired networks. Only in distance-dependent networks it appears that in- and out-neighbors can be considered equivalent in their influence on connection probabilities (Figure 1.16 A-B). Furthermore, while the distribution of the number of common neighbors is consistent in distance-dependent networks, the other network types display a characteristic distribution of common out-neighbors (Figure 1.16 D-E). While the latter observation clearly also relates to the differences in out-degree distributions found in Section 1.2, finding differences between common inputs and outputs in neuron pairs is consistent with the observations of Perin et al., who report a significant difference in effect of the common neighbor rule. In trying to model the inherently asymmetric axonal-dendritic connections between pyramidal cells in cortical circuits with the anisotropic networks, finding such disparity is not only expected but gives the model further validity as an approach to obtain network connectivity going beyond the distance-dependent archetype, which here fails to produce diverging connectivity statistics for in- and outputs.

anisotropy induces  
characteristic  
common neighbor  
rule

Both for in- and out-neighbors, we find characteristic curves describing their influence on connection probabilities. The in-neighbor profiles split into two categories: While networks with anisotropy in connectivity (blue, orange) display a constant increase, distance-dependent network types (red, green) show a sigmoidal shared input-connection probability curve (Figure 1.16 A). We thus find a strong influence of anisotropy on the shared input relationship, inducing a common neighbor rule characteristically different from isotropic, distance-dependent networks.

anisotropy as  
underlying  
connection  
principle!

Does this anisotropy-induced rule reflect the findings in cortical networks? Perin et al. report a linear common neighbor relationship, finding a stronger effect when considering only in-neighbors. Imposing the common neighbor rule on *in silico* networks reflecting a distance-dependency as determined *in vivo*, Perin et al. were then able to reproduce the observed overrepresentation of high edge counts in neuron clusters, identifying the common neighbor effect as an underlying connection principle inducing increased high edge counts in clusters comparable to the profiles shown in Figure 1.14. Showing not only the presence of such an edge count overrepresentation in anisotropic networks, but also finding that only networks featuring anisotropy display an approximately linear relationship between common inputs and connection probability, we identify anisotropy in connectivity as a candidate for an underlying connection principle motivated from neuronal morphology, to induce a common neighbor rule, that may be at the

heart of many of the non-random connectivity statistics observed in local cortical networks.

Extending the analysis of shared inputs in the different network types, we further observe that anisotropy affects the number of common in-neighbors typically observed itself (Figure 1.16 D). We specifically find that increases anisotropy in connectivity induces an increased variance in the distribution of common inputs of a random neuron pair (Figure 1.17). Such increased variance may provide an important advantage in the processing of information, allowing a heightened functional specificity in the network, where many neurons do not share many common inputs, enabling a high variety of functionality, and where few neuron pairs have a high number of shared inputs, strengthening their correlation and thus their capacity to relay related information.

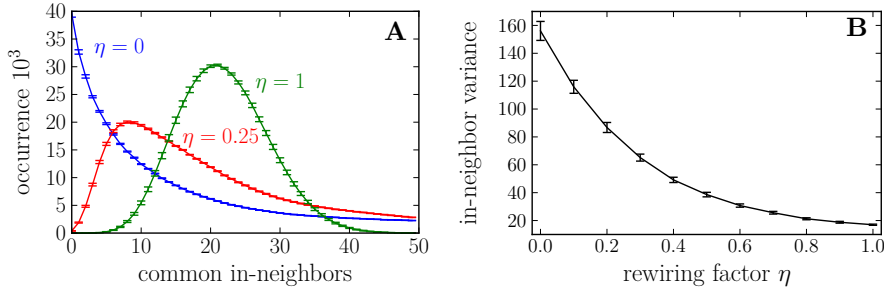


**Figure 1.17: Anisotropy increases variance of common input distribution** Recording common in-neighbor counts for random neuron pairs in tuned anisotropic networks and their rewired versions reveals increased variance in networks with a high degree of anisotropy. **A)** Common in-neighbor distribution for original tuned anisotropic networks ( $\eta = 0$ , blue) and rewired versions with  $1/4$  of all edges rewired ( $\eta = 0.25$ , red) and completely rewired ( $\eta = 1$ , green). (5841710e) **B)** Variance of the common in-neighbor distributions declines with increasing rewiring factor  $\eta$ ; highest variance is found in networks with the highest degree of anisotropy ( $\eta = 0$ ). Errorbars SEM. (ffcefe9b)

## 1.8 DISCUSSION

In their study Perin et al. (2011) were able to relate increased edge-counts in neuron clusters to a *common neighbor rule* - a specific relationship between common in- or outputs in a neuron pair and the probability for the pair to be connected - identifying an underlying principle for the occurrence of non-random connectivity in local circuits. Perin et al. suggest that (fire together wire together). In this structural analysis we found non-random connectivity resembling the findings of Song et al. and , purely from a g. Identifying a common neighbor rule as

the inherent, that non-random connectivity statistics might arise from morphological restrictions rather than plastic processes.